Study of contraction and decontraction processes in the active media of a recombination He–Sr^+ laser

G.D. Chebotarev, O.O. Prutsakov, and E.L. Latush

Rostov State University, Rostov-on-Don

Received November 15, 2005

Using a self-consistent mathematical model of a He–Sr^+ recombination laser developed, we have investigated evolution of the radial distribution of plasma parameters and lasing characteristics in a pulse-periodic regime of the laser operation. The calculations performed show a good agreement with the experimental data. We have also studied, by means of mathematical modeling, the phenomena of contraction and decontraction. It is established that contraction of the pulse-periodic discharge in the pure helium is caused by thermal plasma inhomogeneity formed by a series of pulses. It is shown that self-decontraction of the gas-discharge, when metal atoms are introduced into the pure inert gas, is caused, in the first place, by the low ionization potentials of the strontium atoms. This leads to almost complete double ionization of the strontium atoms practically over the entire cross section of the discharge tube. At the same time, spatial stabilization of the helium ionization process also occurs. As a result, flattening of the radial profile of the electron concentration occurs as the strontium atom concentration increases.

Pulse-periodic metal vapor lasers operate under conditions of a contracted discharge in a pure inert gas.[1–3] The contraction phenomenon makes lots of problems in developing high-power lasers, for it breaks the spatial homogeneity of an active medium.[1–5] To overcome this problem, there are many technical solutions. However, when applied, they complicate a laser system design. At the same time, for the metal vapor lasers (MVL) that contain an inert buffer gas and metal vapor, there is a reverse process of self-decontraction, which yields a high spatial homogeneity of the plasma.[1–3] Therefore, the decontraction phenomenon is of much importance in physics of the metal vapor lasers, and its comprehensive study is definitely of great interest.

The phenomenon of discharge contraction in inert gases has been well investigated by now, the stationary and pulsed volume discharges considered most thoroughly.[4–12] The development of pulse-periodic MVLs has fostered researches into the contraction and decontraction phenomena in a longitudinal pulse-periodic discharge.[1–3,13–15] This discharge has a specific feature in that under conditions of the discharge excitation typical of the MVL, no contraction phenomenon is observed during a single discharge pulse, but it manifests itself at high pulse repetition rates.[3,14] Another specific feature is maintenance of the discharge uniformity in a gas–vapor mixture even under development of near-electrode instabilities or in the presence of contracted discharge segments with depleted metal vapor.[2,3,14]

The phenomenon of discharge contraction in inert gases follows from the ionization-overheating instability and appears when at least two conditions are met simultaneously, i.e., the frequency of charged particle formation must sharply fall off along the radius from the discharge axis to its periphery; volume recombination of charged particles must prevail over the ambipolar diffusion.[4–6]

It is clear that contraction will be surmounted, i.e., the discharge undergoes decontraction, at violation of at least one of these conditions. Gas-discharge conditions that foster decontraction can be realized if an additional easily ionizable impurity takes part in the discharge. A qualitative analysis of decontraction mechanisms of a pulse-periodic discharge in the mixtures of inert gases with metal vapor can be found in Refs. 1–3, 13, and 14. It is shown in these papers that metal vapor, if injected into the discharge at a relatively low concentration (corresponding to the typical MVL lasing conditions), favor the formation of a radial profile of the mixture ionization ability, which grows from axis to tube walls. Thus, the plasma conductivity becomes more uniform over the tube cross section, and the diameter of a discharge channel increases. In Refs. 2, 13, and 15 the authors emphasize the role of residual pre-pulse concentration of electrons in ignition of a uniform pulse-periodic discharge in a gas–vapor mixture. In Refs. 3 and 14, you can find conclusions about the important role of ambipolar diffusion of metal ions, which contributes, along with gas heating, to formation of a non-uniform radial profile of metal vapor density with its minimum on the axis.

This work aims at a detailed numerical investigation into the mechanisms of contraction and decontraction of a pulse-periodic discharge in a He–Sr mixture with the help of our self-consistent mathematical model of a He–Sr^+ laser.

A He–Sr^+ laser belongs to ion recombination metal-vapor lasers.[16–18] It generates in the violet (430.5 and 416.2 nm SrII) spectral region at a high average power (up to several Watts). Its active medium is a mixture of strontium vapor and helium,

0235-6880/06/02–03 99-07 $02.00

the latter serving a buffer gas. The desired density of strontium vapor is reached via heating of the active area. Heating can be performed using an external furnace or by the discharge energy in the self-heating mode. The active medium is excited by short high-power pulses of the electric current, which gives an almost complete double ionization of strontium. This is facilitated by the smallness of potentials of single and double ionization of strontium as compared to the helium ionization potential.

Upon current pulse termination, plasma starts to recombine. Pumping of the upper laser levels is achieved with the impact-radiation recombination of doubly ionized strontium atoms in the afterglow of a pulsed discharge, while inversion is achieved with the effective depopulation of the lower levels of the lasing transition due to de-excitation by electrons. Recombination pumping of the upper laser levels and collisional depopulation of the lower ones are most efficient at a quick and deep cooling of the electron gas at the early stage of the afterglow, what occurs due to elastic collisions of electrons with light helium atoms and ions. For this reason, the enhancement of the helium pressure favors the growth of the lasing energy.

In Ref. 19, we have described the mathematical model of a He–Sr^+ laser we developed. It allows us to calculate the time and energy characteristics of the active medium in a wide range of pressures of the gas mixture. In this work, we used a new self-consistent mathematical model of recombination He–Sr^+ laser, which has made it possible to calculate spatiotemporal evolution of plasma parameters and lasing characteristics in the pulse-periodic mode. The principal distinction of the new model from the one proposed in Ref. 19 is the following. In the kinetic equations for long-lived plasma components we have replaced the diffusion terms of the form $6D/R^2$, where D is the diffusion coefficient and R is the tube radius, by the radial divergences of the density of diffusion fluxes. We also introduced to the electronic and gas temperatures equations the divergences of density of the electronic and gas heat fluxes caused by the heat conductivity of the gas and electrons.

In Ref. 20, the authors measured radial profiles of the electron concentration in both contracted and decontracted pulse-periodic discharges in a He–Sr^+ laser. They also measured the electron temperature. Therefore, we performed our model calculations having in mind the conditions from that paper. For example, the internal diameter, the active length, and the pulse repetition rate were, respectively, $d = 1.55$ cm, $L_a = 70$ cm, and $f = 6$ kHz.

The calculated spatiotemporal dependences of plasma parameters and lasing characteristics of a He–Sr^+ laser in a stationary pulse-periodic mode are presented in Fig. 1. Figure 1*a* shows the calculated and experimental (Ref. 20) radial profiles of electron concentration at different time moments with respect to the moment when current maximum is achieved. Figure 1*b* shows the calculated and experimental profiles of electron temperature during afterglow at the moment of lasing maximum.

The calculated spatiotemporal dependences of electron and gas temperature, atomic concentration, single and double strontium ions, and the lasing intensity at 430.5 nm for SrII are shown in Figs. 1*c*–*h*. We can see that in the stationary mode, gas temperature during a single current pulse varies insignificantly (Fig. 1*d*). It is non-uniform over the radius, which, along with the ambipolar diffusion, results in a non-uniform pre-pulse radial distribution of metal atoms (Fig. 1*e*). The profile of double ions of strontium at the end of a current pulse (Fig. 1*g*) almost follows the pre-pulse profile of strontium atoms (except for thin near-wall region), which undergo almost complete double ionization during the pulse. The dip in the concentration radial profile of the double ions of strontium on the axis gives the minimum in lasing intensity on the tube axis (Fig. 1*h*). The radial profile of the intensity with a small dip on the axis is quite typical for a He–Sr^+ laser and was observed both in our experiments and in the studies by other authors.[2,21]

As seen in Fig. 1, this model quite accurately describes the main regularities in the behavior of the characteristics of the active medium of a He–Sr^+ laser.

Figure 2 shows the steady-state radial profiles of electron concentration and gas temperature as well as of a pre-pulse concentration of helium atoms for a discharge in pure helium calculated for different pulse repetition rates.

It can be seen that at low rates ($f \sim 10^2$ Hz), the radial profile of gas temperature is close to a uniform one (Fig. 2*c*), and the profile of electron concentration tends to the besselian profile, which is characteristic of a non-contracted discharge (Figs. 2*a* and *b*). At higher rates (above 10^3 Hz), thermal non-uniformity of plasma starts growing abruptly (Figs. 2*c* and *d*), that causes narrowing of the electron concentration profile and growth of its values on the discharge axis via ionization overheating. The calculated profile of N_e at $f = 6$ kHz is close to the experimental one for a contracted discharge (Ref. 20), Figs. 2*a* and *b*.

Figure 3 illustrates the radial distributions of plasma parameters in different pulses. For the initial conditions for the first pulse we took, as seeding, the uniform distributions of all plasma parameters. Up to the 60th pulse, the discharge was modeled in a pure helium medium and then after the strontium atoms were added.

It can be seen that, first, the discharge is not contracted. Its contraction occurs after about 40 pulses. This number of pulses corresponds to the time needed for a temperature regime to settle (~ 6 ms). From Figs. 3*e* and *f*, we see that, first, when the gas has just started warming, helium concentration is not so quick in responding to a temperature change, it needs about $\tau_{diff} = R^2/6D_{He} \approx 4$ ms. This makes helium pressure to increase, for $p_{He} \propto N_{He}T_g$. Gas temperature setting time is determined by the characteristic time $\tau_{th} = R^2/6\chi \approx 2$ ms, where χ is the coefficient of helium thermal conductivity. The parameters T_g and

N_{He} in transfer equations are interrelated. Therefore, the time needed to settle will equal to the sum of the times $\tau_{diff} + \tau_{th} \approx 6$ ms. In a steady-state regime, helium pressure is radially constant (Fig. 3*f*), and a pre-pulse profile of helium concentration is inverse to the profile of gas temperature (Fig. 3*e*).

A decrease in helium concentration on the axis because of the gas heating favors the growth of T_e on the axis (Fig. 3*b*), because $T_e \propto E/N_{He}$, where E is the field strength. Because of high excitation and ionization potentials of helium, its ionization rate is very sensitive to the drops in T_e along the tube radius. That is why the ionization rate of pure helium is highest on the axis. Consequently, N_e (Fig. 3*a*) and plasma conductivity (Fig. 3*d*) on the axis increase sharply, i.e., the discharge gets contracted.

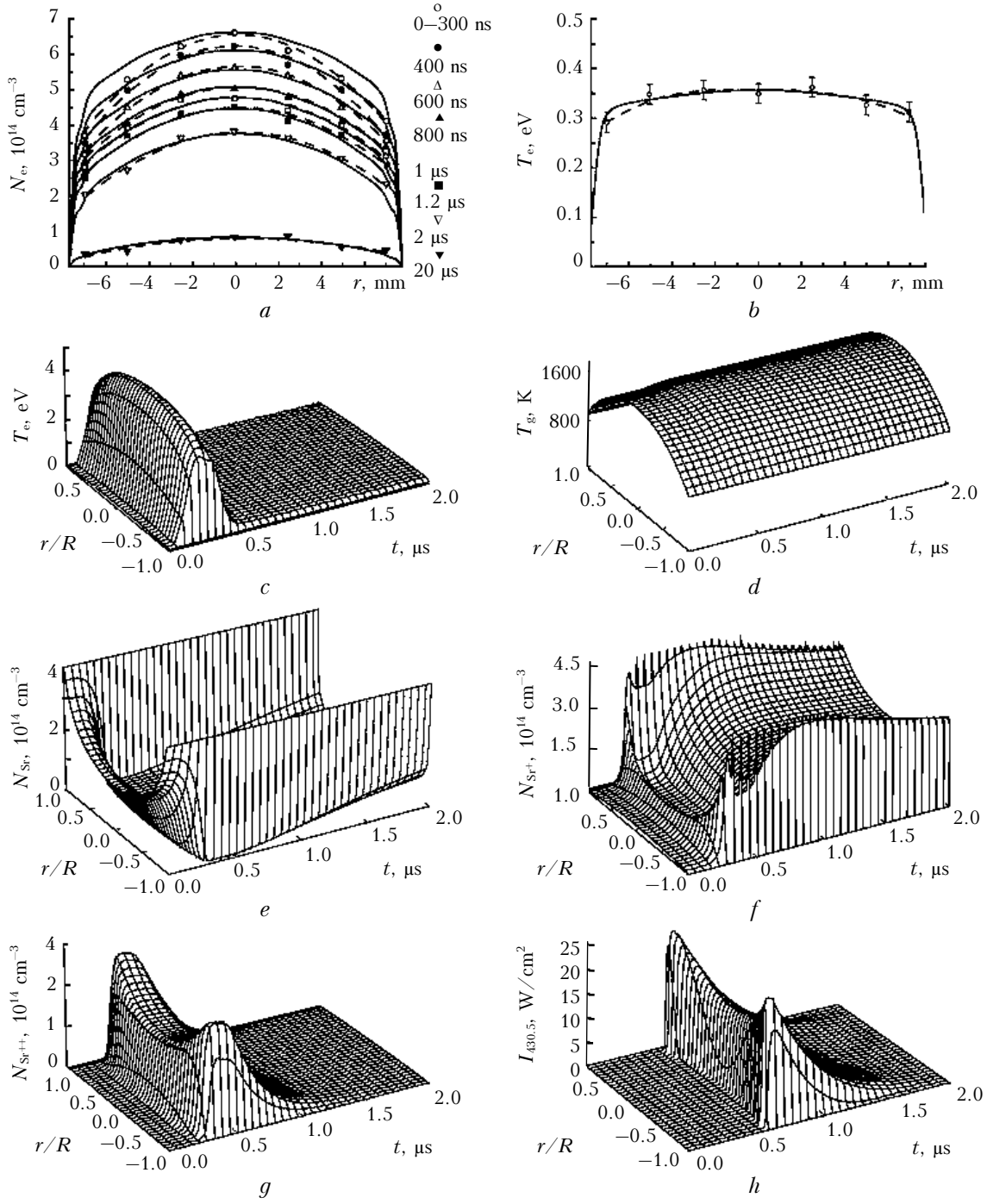

Fig. 1. Radial profiles of electron concentration at different time moments with respect to the moment when the current maximum is achieved (*a*), the radial profile of electronic temperature at the moment of lasing maximum (*b*), spatiotemporal dependences of electron temperature (*c*), gas temperature (*d*), atomic concentration (*e*), single (*f*) and double (*g*) ions of strontium, and the lasing intensity at 430.5 nm of Sr II (*h*): p_{He} = 250 Torr; dashed curves present experimental values.

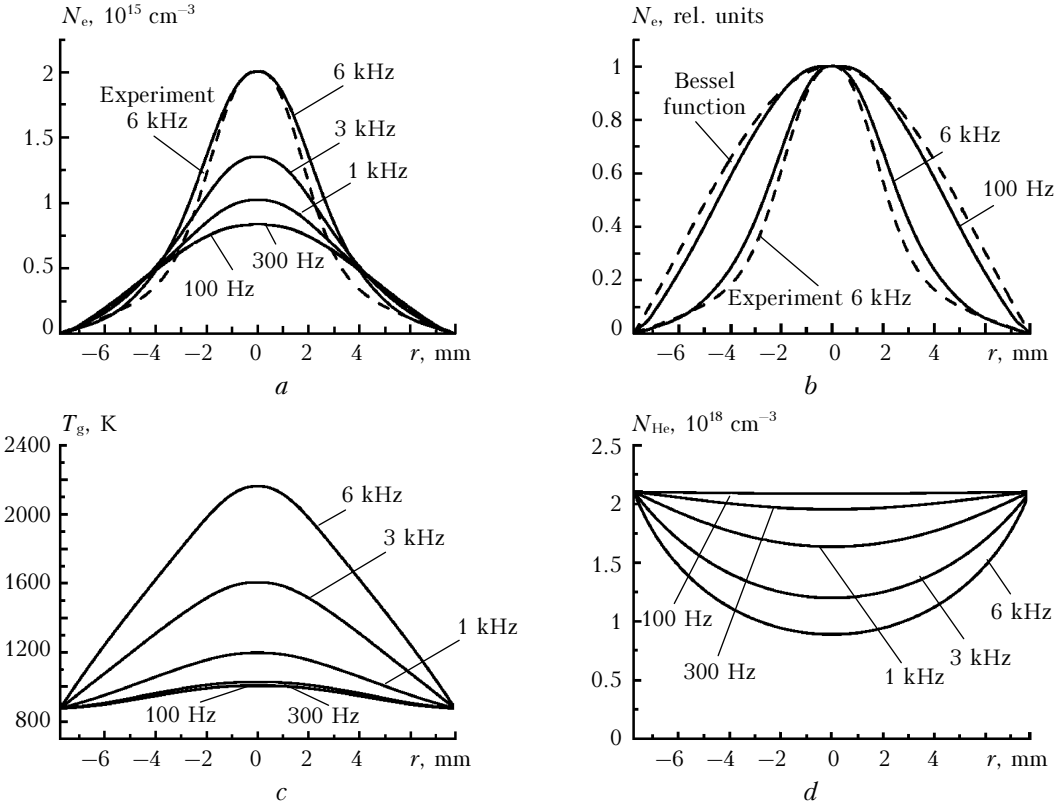

Fig. 2. Radial profiles, at their maxima of electron concentration (*a*, *b*), gas temperature (*c*), and a pre-pulse concentration of helium atoms (*d*) at a discharge rate in a pure helium of p_{He} = 190 Torr.

The energy of only one current pulse is not enough to considerably heat the gas. Therefore, in a single pulse, the discharge does not undergo any noticeable contraction. However, in a pulse-periodic mode, when $1/f \ll \tau_{diff} + \tau_{th}$, the heat is accumulated from pulse to pulse until the radial distribution of T_g reaches the stationary mode with a pronounced axial maximum (Fig. 3*c*). A temporal plasma inhomogeneity that develops in a series of pulses finally results in the discharge contraction (Figs. 3*a* and *d*).

The modeled regularities in the behavior of a pulse-periodic discharge in helium agree with our experimental results and the results in Refs. 2, 3, 13, 14, and 20.

Figure 3 illustrates the process of decontraction due to addition of strontium atoms ($N_{Sr} = 4 \cdot 10^{14}$ cm^{-3}). In the model, they were introduced into the discharge with the 60th pulse. We can see that decontraction occurs rapidly. By the 70th pulse, the discharge has been fully decontracted, with gas and electron temperatures, electron concentration, and plasma conductivity reduced on the axis. Radial distributions of N_e and plasma conductivity become nearly flat.

Figure 4 shows the steady-state radial distributions of plasma parameters at the end of the current pulse, when N_e is the highest. These distributions were calculated for different amounts of the strontium atoms added.

We can clearly see decontraction of the discharge if adding an easily ionizable substance. The added strontium starts manifesting its effect at a concentration of $\sim 5 \cdot 10^{13}$ cm^{-3}. At $N_{Sr} = 4 \cdot 10^{14}$ cm^{-3}, radial distribution of electrons becomes nearly flat (Fig. 4*a*).

We see that in a current pulse almost all metal atoms undergo ionization. Most of them change to double ions (Figs. 4*b* and *c*). The radial profile of double metal ions almost reproduces a pre-pulse profile of strontium atoms (except for thin near-wall tube region), which are more abundant at the walls than on the axis (this is due to thermal and ambipolar diffusion). Note that low potentials of single and double strontium ionization play a key role in effective ionization of strontium in the near-wall areas along with the described shape of a pre-pulse profile of strontium atoms. Low ionization potentials result in a much lower sensitivity of metal ionization rate, as compared to helium, to drops of T_e along the tube radius (Fig. 4*e*).

The growth of N_e and of plasma conductivity in the near-wall region (Figs. 4*a* and *g*) that accompanies the increase in strontium concentration leads to a more intense heat release near tube walls and its weaker release on the axis, the latter assumes constancy of the pump power. Thus, the heat-release profile smoothed out. In its turn, this results in a considerable decrease in gas temperature in the axial part of the discharge and some its growth near the walls (Fig. 4*f*). These changes in the gas temperature profile as well as the increased energy losses of the

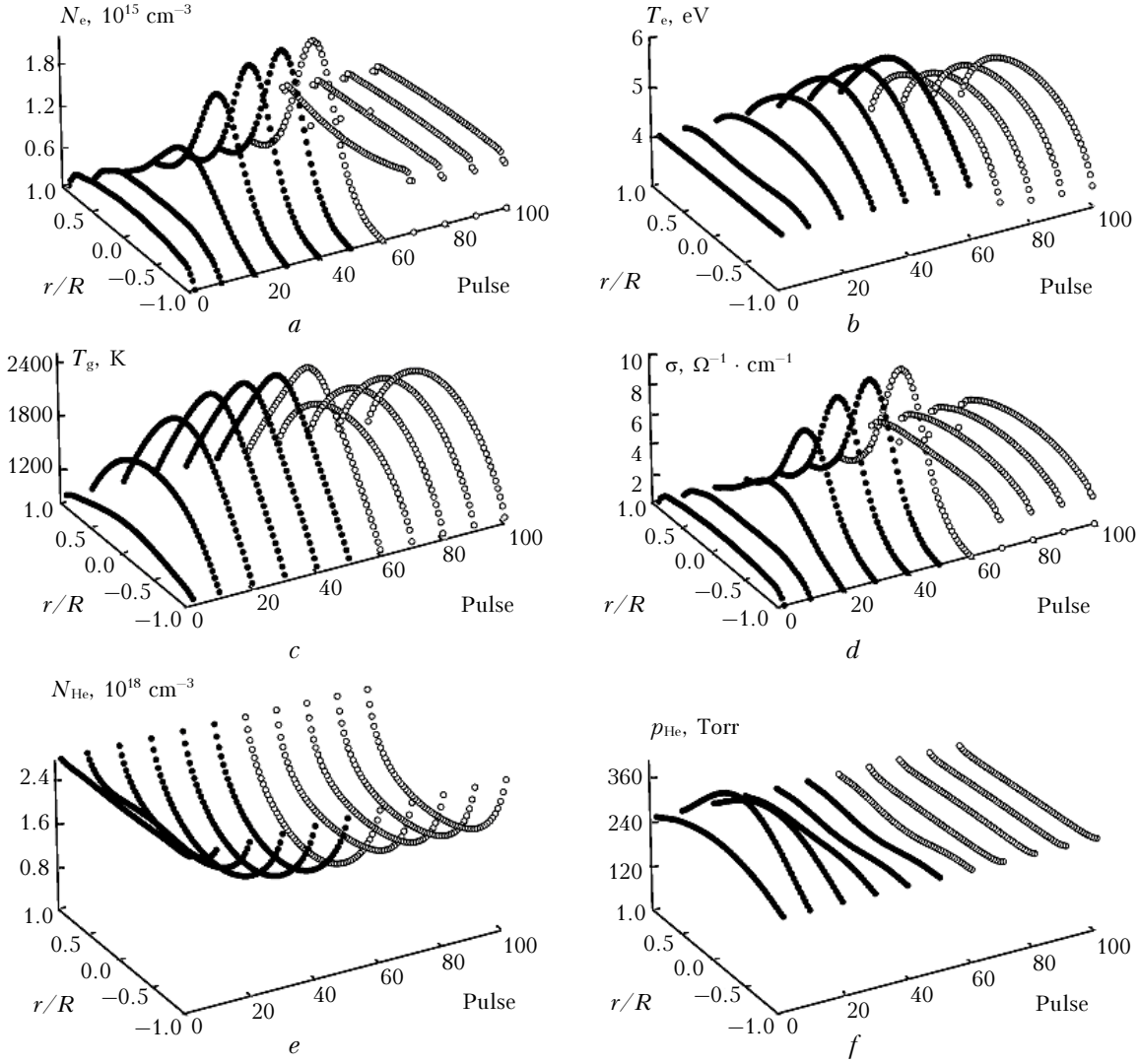

Fig. 3. Radial profiles, at their maxima of electron concentration (*a*), electron temperature (*b*), gas temperature (*c*), plasma conductivity (*d*), and pre-pulse radial distributions of helium concentration (*e*) and helium pressure (*f*) in different pulses; through the sixtieth pulse, the discharge is burning in a pure helium, then strontium is added in the amount of $4 \cdot 10^{14}$ cm^{-3}; p_{He} = 190 Torr.

electron gas occurring due to strontium ionization result in some decrease in the electron temperature and reduce its drops along the tube radius (Fig. 4*e*). In its turn, this strongly smoothes out the radial profile of helium ion concentration, due to strong dependence of helium ionization rate on T_e (Fig. 4*d*). Thus, adding an easily ionizable substance, among the other effects, stabilizes the ionization process of buffer gas, whose ions, together with single and double metal ions, greatly contribute to the resulting radial profile of electron concentration (Figs. 4*a–d*).

Note an interesting detail: the radial profile of N_e, which becomes nearly flat at a certain concentration of strontium, is determined by non-uniform concentration profiles of different ions in a gas–vapor mixture (Figs. 4*a–d*).

Figure 4*h* presents the total rate of all the ionization processes in a He–Sr mixture that lead to formation of charged particles and include a direct and a stepwise ionization. As seen from Fig. 4*h* (which illustrates evolution of the radial profile of the mixture ionization properties), the increase in strontium concentration violates one of the conditions for contraction to occur, namely, a sharp decrease in charged particle formation rate from tube axis to walls; as a result, contraction is neutralized and the discharge decontracts back.

As calculations show, a pre-pulse concentration of electrons in a steady-state pulse-periodic discharge for such composition of a He–Sr mixture that corresponds to a uniform radial profile of N_e is equal to ~ 10^{13} cm^{-3}, which is several orders of magnitude higher than the values required for formation of a volume discharge.[2,15]

Our calculations for largely varied concentrations of mixture components show that, to maintain a high spatial homogeneity of plasma at an increasing helium pressure, we need to increase the concentration

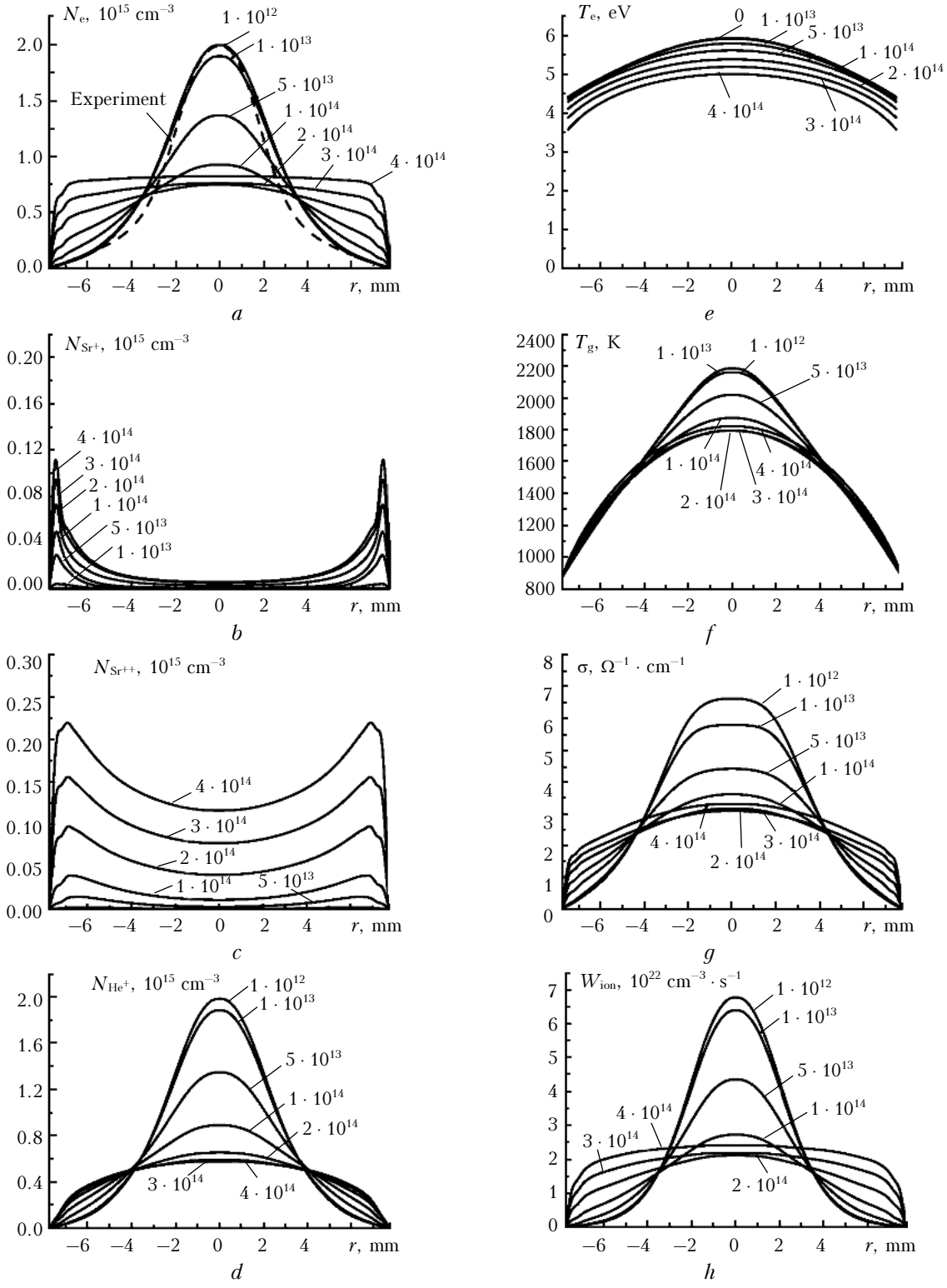

Fig. 4. Radial profiles, at a current pulse end, of electron concentrations (*a*), single strontium ions (*b*), double strontium ions (*c*), helium ions (*d*), electron temperature (*e*), gas temperature (*f*), plasma conductivity (*g*), total helium and strontium ionization rate (*h*): $p_{He} = 190$ Torr. Dashed curve corresponds to the experiment. Numbers accompanying curves are values of atomic strontium concentration at tube walls, in cm^{-3}.

of strontium atoms (and increase the energy input to the discharge). Here, the mixture component ratios that would be the best for attaining the maximum possible plasma homogeneity are close to the ratios that yield the highest rate of recombination pumping of ion levels of strontium and, correspondingly, the

highest energy characteristics of lasing of a recombination He–Sr^+ laser. This feature promotes a fast growth of pulsed energy characteristics of a He–Sr^+ laser at the increase in helium pressure up to several atmospheres.[22] The mentioned relation between mixture composition and plasma homogeneity is observed experimentally for the He–Sr mixture and for other mixtures as well.[2,3]

The calculations also show that at a fixed helium pressure and strontium concentration increasing within one order of magnitude, plasma remains homogeneous enough, which enables an effective self-terminating lasing in a He–Sr mixture on the atomic and ion transitions in strontium in the infrared spectral region with the best mixture composition, which is slightly different from that of a recombination laser.[23]

Thus, using the method of mathematical modeling, we have investigated the phenomena of contraction and decontraction of a pulse-periodic discharge important in the physics of metal-vapor lasers. We have established the main physical mechanisms that determine existence of these phenomena.

Acknowledgments

The work was supported by the Russian Foundation for Basic Research (Grant No. 04–02–96804).

References

1. L.M. Bukshpun, E.L. Latush, and M.F. Sem, Sov. J. Quant. Electron. **18**, No. 9, 1098–1100 (1988).
2. P.A. Bokhan and D.E. Zakrevsky, Zh. Tekh. Fiz. **67**, Issue 4, 25–31 (1997).
3. V.M. Klimkin, *"Instability of longitudinal pulse-periodic discharges in metal vapor lasers,"* Preprint No. 1, IAO SB RAS, Tomsk (1999).
4. Yu.P. Raiser, *Gas Discharge Physics* (Nauka, Moscow, 1987), 592 pp.
5. A.V. Eletsky and B.M. Smirnov, Usp. Fiz. Nauk **166**, No. 11, 1197–1217 (1996).
6. E.P. Velikhov, A.S. Kovalev, and A.T. Rakhimov, *Physical Phenomena in Gas-Discharge Plasma* (Nauka, Moscow, 1987), 160 pp.
7. Yu.D. Korolev and G.A. Mesyats, *Pulsed Breakdown Physics of Gases* (Nauka, Moscow, 1991), 224 pp.
8. V.V. Osipov, Usp. Fiz. Nauk **170**, No. 3, 225–245 (2000).
9. Yu.B. Golubovsky, V.O. Nekuchaev, and E.B. Pelyukhova, Zh. Tekh. Fiz. **66**, Issue 3, 43–53 (1996).
10. Yu.S. Akishev, A.P. Napartovich, S.V. Pashkin, V.V. Ponomarenko, N.A. Sokolov, T.V. Taran, and M.D. Taran, Fizika Plazmy **10**, Issue 2, 361–371 (1984).
11. K.N. Ulyanov, Zh. Tekh. Fiz. **43**, Issue 3, 570–578 (1973).
12. G.M. Petrov and C.M. Ferreira, Phys. Rev. E **59**, No. 3, 3571–3582 (1999).
13. P.A. Bokhan and D.E. Zakrevsky, Pisma Zh. Tekh. Fiz. **62**, Issue 1, 26–30 (1995).
14. V. Klimkin, Proc. SPIE **4747**, 164–179 (2002).
15. V.M. Klimkin, Pisma Zh. Tekh. Fiz. **29**, Issue 18, 16–21 (2003).
16. I.G. Ivanov, E.L. Latush, and M.F. Sem, *Metal Vapor Ion Lasers* (Energoatomizdat, Moscow, 1990), 256 pp.
17. I.G. Ivanov, E.L. Latush, and M.F. Sem, *Metal Vapor Ion Lasers: Kinetic Processes and Gas Discharges* (John Willey & Sons, Chichester, New York, 1996).
18. C.E. Little, *Metal Vapor Lasers: Physics, Engineering and Applications* (John Willey & Sons, Chichester, New York, 1999).
19. G.D. Chebotarev, O.O. Prutsakov, and E.L. Latush, Proc. SPIE **5483**, 83–103 (2004).
20. D.G. Loveland and C.E. Webb, J. Phys. D **25**, 597–604 (1992).
21. C.E. Little and J.A. Piper, IEEE J. Quantum Electron. **26**, No. 5, 903–910 (1990).
22. S.N. Atamas', E.L. Latush, and M.F. Sem, J. Russian Laser Res. **15**, No. 1, 66–68 (1994).
23. A.N. Soldatov, Yu.P. Polunin, A.S. Shumeiko, and I.V. Sidorov, in: *Abstracts of Reports at Symp. on Metal Vapor Lasers*, Rostov-on-Don (2004), p. 18.